

# Modeling and optimizing phenol degradation in aqueous solution using post discharge DBD plasma treatment

Nura Nafe Ali <sup>a</sup>, Haiyam M. Alayan <sup>a</sup>, Adnan A. AbdulRazak <sup>a,\*</sup>, Rana R. Jalil <sup>b</sup>

<sup>a</sup> Department of Chemical Engineering-University of Technology, Baghdad, Iraq

<sup>b</sup> Petroleum Research and Development Center, Ministry of Oil, Bagdad, Iraq

## ARTICLE INFO

### Keywords:

Dielectric barrier discharge  
Nonthermal plasma  
Phenol  
Degradation  
Wastewater treatment, response surface methodology

## ABSTRACT

The present study was carried out to optimize the treatment process of phenol in aqueous solution using dielectric barrier discharge (DBD) plasma and experiments were designed by using response surface methodology and central composite design (RSM-CCD). The study explores the efficacy of a DBD plasma system that mainly generates ozone in the degradation of phenol in standard aqueous solutions at concentrations simulating those found in industrial wastewater from operating units in Iraqi oil refineries. The study investigates the influence of key operating factors, namely, applied voltage (Volt), air flow rate (L/min), initial phenol concentration (ppm), and treatment time (min) aiming to identify the removal efficiency optimal conditions. According to the analyzed results of RSM, the experimental data is best fitted with a model of the quadratic polynomial with regression coefficient values of more than 0.9. After 10 minutes, almost 50 % of phenol with an initial concentration of 4 ppm was eliminated. Optimal degradation of phenol was achieved by elevating the voltage from 10,000 to 30,000 V. The % phenol degradation increased from 0 % to 82 %. With the right conditions—an initial phenol concentration of 2.47 ppm, a flow rate of 0.50 L/min, a time of 14.53 min, and an applied voltage of 29,986.38 volts—under these optimal conditions, a phenol removal efficiency of 97.5 % was achieved. The Pareto chart confirmed that the time and the applied voltage have the greatest influence on the % phenol degradation. Additionally, we showed that DBD had the highest removal efficiency with hydroxyl radical playing the major role in the degradation while O<sub>3</sub>-DBD also gave rise to relatively high efficiency with ozone making an important contribution. The findings of this study underscore the immense potential of non-thermal discharge plasma technology and the utilization of RSM in enlightening the optimization of advanced oxidation processes for effective wastewater treatment.

## 1. Introduction

Water pollution diminishes water quality and reduces access to potable water [1,2], Industrial waste, agricultural runoff, urban runoff, and natural disasters are among the many potential sources of water contamination. These pollutants pose a threat to aquatic ecosystems as well as human health [3].

The volume of wastewater containing various refractory organic contaminants has expanded substantially in recent years due to the rapid development of the petrochemical, paper, coking, printing, and dyeing sectors [4]. The wastewater from the petroleum sector contains a variety of contaminants, including petroleum hydrocarbons, mercaptans, oil and grease, phenol, ammonia, sulfide, and other organic compounds. All of these chemicals exist in highly complex forms in the petroleum

sector's effluent, causing direct or indirect environmental hazards [5]. Numerous publications have reported the detection of multi-ring aromatic hydrocarbons in various groundwater sources. Table 1 shows the Characteristics of typical petroleum refinery wastewater reported from the literature. The United States Environmental Organization has focused on these chemicals because of their toxicity and carcinogenic potential for humans and many animal species [6].

The petroleum refining sector consumes substantial quantities of water. The water requirement reaches 3.0 m<sup>3</sup> for each ton of petroleum refined. In compliance with environmental regulations that enforce particular limits on pollutant emissions and to supply adequate water for oil refineries engaged in crude oil processing, this water may also serve many functions. These encompass fire suppression, irrigation, aquifer recharge, vehicle cleaning, and cooling water for power generation

\* Corresponding author.

E-mail address: [adnan.a.alsalim@uotechnology.edu.iq](mailto:adnan.a.alsalim@uotechnology.edu.iq) (A.A. AbdulRazak).

<https://doi.org/10.1016/j.dwt.2025.100993>

Received 30 November 2024; Received in revised form 2 January 2025; Accepted 7 January 2025

Available online 8 January 2025

1944-3986/© 2025 The Author(s). Published by Elsevier Inc. This is an open access article under the CC BY license (<http://creativecommons.org/licenses/by/4.0/>).

plants [23]. These considerations have generated a significant economic impetus to optimize water usage and heightened the necessity for improved water management and wastewater reduction [24]. Consequently, industrial water produced by oil refineries can be regarded as a significant human resource for acquiring substantial volumes of water to satisfy public and individual requirements, provided it is treated appropriately, efficiently, and cost-effectively. Petroleum wastewater can vary considerably depending on the facility configuration, operational techniques, and the specific type of oil being processed [25].

Three types of treatments exist for petroleum wastewater: Physical, chemical, and biological. However, the complex properties of petroleum effluent necessitated the standard implementation of an integrated system for the treatment. Consequently, traditional treatment procedures require a multistage processing approach [26]. In recent years, numerous advancements in technological methodologies for both advanced treatment and pre-treatment have been implemented, with the exception of physical separation, owing to its efficacy in petroleum wastewater management. Several methods, including ionizing radiation, non-thermal plasma, Anodic oxidation, carbon adsorption, advanced oxidation processes (AOPs), ozone oxidation, and sonolysis, are preferred for getting rid of harmful substances in contaminated water [27,28]. Recent research indicates that strategies involving carbon nanotubes magnetized by nano zero-valent iron are effective in improving the removal of contaminants such as nitrates from aqueous solutions [29]. This method shows how nanomaterials might be used to improve the removal of pollutants, similar to how cold plasma technology can be improved for breaking down phenol. AOPs are significant methodologies that are favored over alternative procedures. These approaches do not produce detrimental sedimentation nor transform contaminants from one phase to another, the AOP is a type of clean technology, wherein water pollutants are converted into CO<sub>2</sub> and H<sub>2</sub>O. AOPs produce large numbers of OH• radicals for decomposing an extensive range of chemical compounds (e.g. halogenated hydrocarbons, pentachlorophenol, pesticides, herbicides, aromatic compounds, and more recently pharmaceuticals) [30]. Due to their high reactivity, OH• radicals provide an effective means of decomposing complex toxin structures using a series of chemical reactions. However, conventional advanced oxidation is not one of the best available or most cost-effective treatment techniques due to its requirement for additional equipment. To overcome these issues, a cost-friendly, versatile means of OH• radical production that has been attracting increasing interest is plasma technology. The latest studies on wastewater treatment at petroleum fuel filling stations have demonstrated the possibility of integrating effective treatment technologies to recycle contaminated wastewater, particularly for cooling towers at petroleum refineries [31]. Recently,

non-thermal or low-temperature plasma (NTP or LTP) technology has been introduced for the treatment of plenty of pollutants and has received increasing attention due to the advantages such as high efficiency, simplicity, no secondary pollution, and environmental protection effect [32]. Generally, non-thermal plasma discharge can effectively degrade environmental pollutants because it can produce a series of active particles including reactive radicals, oxidizing molecules, and hydrated electrons, as well as ultraviolet radiation, which all may trigger complex chemical reactions to destroy the pollutants [33]. Non-thermal plasmas have been achieved under normal atmospheric pressure by avoiding gas heating with the help of dielectric barrier discharge (DBD). DBD plasma reactor is an example of a non-thermal plasma technique having one or more dielectric layers placed between the electrodes. This reactor is very efficient as it can produce ozone along with UV radiation and radicals (e.g., OH•), excited atoms (e.g., O•), molecules, electrons, and ions. Ozone is a potential oxidant (E<sub>0</sub> = 2.07 V) and reacts with many organic compounds via direct or indirect reactions.

Phenolic chemicals are recognized disinfectants and sterilizers, as well as precursors for synthetic resins, colors, medicines, fragrances, insecticides, tanning agents, solvents, and lubricating oils. Prolonged exposure to phenol results in paralysis of the human central nervous system and causes damage to the kidneys and lungs [34]. They are the representatives of water solubility and are classed as both a teratogenic and carcinogenic agent. Phenol biodegradability in surface waters reaches only 90 % after seven days, while the aquatic toxicity of phenol is 12 mg/L [35]. The elimination of phenolic compounds from petroleum refineries wastewater is a critical and pressing issue and has to meet the Environmental Protection Agency's (EPA) effluent limits of 0.1–1 mg/L for phenol concentrations.

Therefore, in this study, we prioritize the investigate of the efficacy of DBD cold plasma as a viable and alternative method for the removal of phenol from water. This study aims to extend the practical applications of non-thermal plasma in the treatment of phenolic-contaminated water, highlighting the implication of plasma-generated gases in wastewater treatment. A green approach that utilizes DBD plasma with ambient air as the feeding gas was used to generate reactive species such as O<sub>3</sub>. In this mode, the discharge occurs in the absence of water or water vapor in the reactor. Then, the exhaust plasma gas is brought into contact with the solution to be treated in a bubbler. In response to the large interfacial area and intense liquid agitation, bubbly flows of exhaust plasma gas led to a high mass transfer rate between active species from the gas to the liquid. Unlike previous studies, which used electrical discharges generated in or in contact with water, using post-discharge configuration, the atmosphere inside the reactor is not affected by the evaporation of

**Table 1**  
Characteristics of typical petroleum refinery wastewater reported from the literature.

Parameters										
pH	BOD (mg/L)	COD (mg/L)	TSS (mg/L)	TDS (mg/L)	TOC (mg/L)	NH <sub>3</sub> (mg/L)	Phenols (mg/L)	Sulfides (mg/L)	Oil and Grease (mg/L)	References
7.74	155	485	600	800	-	13.7	3.5	-	17.36	[7]
-	1198	2554	-	-	610.93	81.2	-	-	-	[8]
6.7	174	450	150	-	119	-	-	-	870	[9]
8.3–8.9	-	3600–5300	30–40	3.8–6.2	-	-	11–14	-	-	[10]
9.2	-	970	42.3	1220	-	-	-	-	-	[11]
7.2	107.3	232.7	86.2	276	-	0.7	0.17	-	2.9	[12]
8.0	718	1494	75	-	-	-	70	142	-	[13]
8.0	195	480	315	-	-	-	13.8	16.8	94	[14]
8.3–8.7	-	3970–4745	30–40	3800–6200	-	-	8–10	-	-	[15]
7.82	-	310	-	1910	-	-	-	-	-	[16]
8.2	23	-	31	-	-	0.81	20.7	-	-	[17]
7.8	44,300	74,800	2010	41,600	5490	-	-	-	-	[18]
7.3	-	330	253.3	-	391	9.5	-	-	-	[19]
7.2	-	1179	-	74	-	-	257	0.18	217	[20]
8.0	138	350	60	2100	-	-	7.35	-	14.75	[21]
8.0	8.6	112	-	930	-	0.7	-	-	-	[22]

water. Therefore, only gaseous long-life species (i.e. O<sub>3</sub>) are responsible for the degradation of phenol. The impact of various parameters, including the input voltage, initial phenol concentration, air flow rate, and exposing time was investigated using the central composite design (CCD-RSM) method. The optimal operating conditions for maximum phenol removal were also determined, and an empirical model correlating the phenol degradation efficiency to the four variables was then developed. The practical application of the results of this study is related to phenol in industrial wastewater from the Daura refinery in Iraq.

## 2. Material and method

### 2.1. Materials

The phenol crystals were obtained from (Loba Cheme, India) with physical properties presented in Table 2.

### 2.2. Instrumentation

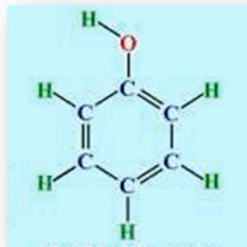
Instrumentations needed in this study are a dielectric barrier discharge (DBD) reactor, oscilloscope, HV probe, clampmeter, AC power supply, and UV-Vis spectrophotometer.

### 2.3. DBD plasma system and operation

The dielectric barrier discharge (DBD) reactor for phenol oxidation consists of two components. Fig. 1 shows the main component. The plasma section, which consists of a Pyrex tube with an inner diameter of 3 cm and a wall thickness of 0.1 cm, is vertically located in the center line of the reactor. The inner electrode, which is a copper rod with a diameter of 2 cm, and the outer electrode, which is a type 304 copper wire mesh, surrounds the Pyrex tube, acting as an insulator and separating the two electrodes. There is a gap of about 1 cm between the two electrodes, with the outer electrode painted black to prevent electron leakage and enhance the aesthetic homogeneity of the system. The high power applied to the reactor was generated by an external 50 Hz AC

**Table 2**  
Physical properties of Phenol.

Physical Properties	Value
Molecular formula	C <sub>6</sub> H <sub>5</sub> OH
Molecular weight (g/mole)	94.11
Purity (GC area %)	Min (99.5 %)
Solubility	5 % in water Clear, Colorless Solution
Freezing point	40.5-41°C
Packed under	Nitrogen
Structural formula	



Phenol crystals



power supply with a peak voltage of 10,000–30,000 Volt. The power supply provides the input voltage to the plasma generator. An airflow meter was used to control the air level between (0.5–1.5) L/min entering the DBD reactor at a specified flow rate. The subsequent part is a bubble column with a diameter of 3 cm, a height of 30 cm, and a width of 2.5 cm. The reactors are connected by a plastic tube that allows ozone and other gases generated in the plasma reactor to pass into the reactor into which a sample liquid (25) ml containing phenol is placed. The generation of O<sub>3</sub> is detected by the typical ozone smell and a glowing violet light. A condenser is located at the top of the system to prevent evaporation and is connected to a cooler at the bottom through plastic tubes. When the voltage across the electrodes exceeds the air level voltage, it leads to the generation of plasma, i.e., the production of fresh ozone and other gases, in addition to oxygen and nitrogen.

### 2.4. Experimental procedure

Several concentrations were prepared according to the experimental operating conditions from the standard solution which was prepared by dissolving 0.25 g of phenol in 250 ml of deionized water. The pH of the sample was 6.5 which is equal to the pH of the polluted water resulting from the operational units of the Daura refinery. All the experiments were conducted using a 25 ml solution of the prepared phenol which was placed into the bubble column reactor. Then Air was pumped into the DBD reactor and controlled by the air flow meter. The pilot power supply for the reactor comprised a Variac transformer adjustable manual voltage regulator. The Variac variable transformer allowed for adjustable output voltages and provided a constant frequency of 50 Hz. When the voltage between two electrodes exceeds the air's voltage level, the plasma is generated. It could swiftly and consistently produce ozone, oxygen, and other reactive species. Then the produced O<sub>3</sub> is introduced to the reactor's base to contact the phenol model fluid, conducting the phenol oxidation process under standard atmospheric pressure and ambient temperature. Previous research has indicated that several factors can significantly influence plasma treatment processes, including the applied voltage, initial concentration of the phenol, air flow rate, and treatment time. Therefore, in this study, these factors were considered as significant variables, and their ranges were carefully selected to ensure complete investigation of their effects on pollutant removal. We computed the subsequent parameters using the data we acquired from the plasma reactor. Table 3 shows the ranges of and the operated factors.

### 2.5. Analytical methods

To assess the phenol concentration throughout the treatment process, samples were regularly collected and analyzed for absorbance at approximately 270 nm ( $\lambda_{max}$ ) using a spectrophotometer and the concentration of phenol could be calculated based on the standard curve. A treated sample (25 ml) was taken at predictable times (5–15 minutes), and the absorbance was documented. The concentration was determined using the Beer-Lambert law. Most of the experiments were performed in duplicate or triplicate, and average data are reported. The degradation percentage was calculated by using the following equation:

$$\% \text{Phenol degradation} = \frac{C_0 - C}{C_0} \times 100 \quad (1)$$

where C<sub>0</sub> and C represent the phenol concentration at initial and various observation times respectively.

### 2.6. Ozone generation

In the DBD reactor, the ozone generation process consists of two stages: initially, energetic electrons (e) generated by electrical discharge collide with oxygen molecules, resulting in their splitting into oxygen

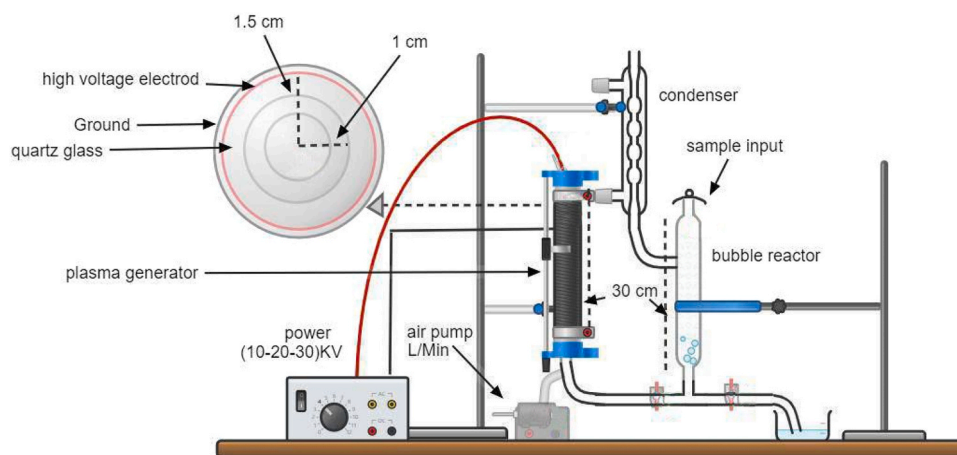


Fig. 1. Schematic diagram of dielectric barrier reactor.

Table 3

Range of experimental variables.

Time (min)	5, 10, 15
Flow rate (L/min)	0.5, 1, 1.5
Applied voltage (Volt)	10,000, 20,000, 30,000
Phenol initial concentration (ppm)	2, 4, 6

atoms. Subsequently, these oxygen atoms collide with oxygen molecules, leading to the formation of ozone. Eqs. (2) and (3) represent the stages of the reaction.



where M is a third collision partner including O, O<sub>2</sub>, or O<sub>3</sub> [36].

### 2.7. Mechanism of phenol degradation via ozone

Ozone is a forceful oxidizing agent capable of reacting with several species that possess multiple bonds (e.g., C=C, C=N, N≡N, etc.). Water and wastewater treatment, disinfection, bleaching, and industrial

oxidation processes extensively use it. The practical applications derive from the considerable oxidizing capacity of ozone. The ozonation of water and wastewater is executed by distributing ozone gas into the liquid phase. Numerous water and wastewater treatment applications have utilized ozone as an oxidant. Ozone is theoretically capable of oxidizing inorganic substances in elevated oxidation states while converting organic components into carbon dioxide and water. There are two potential mechanisms for oxidation in an ozonation process: the direct method and the radical method. Ozone reacts directly with phenol molecules, cleaving the ring to ultimately produce an organic acid molecule, as illustrated in Fig. 2 [37]:

Simultaneously, the radical pathway occurs due to interactions between the generated radicals, particularly hydroxyl radicals OH•, which are formed during ozone decomposition and react with the dissolved compounds. The reaction rate of OH• is 10<sup>6</sup> to 10<sup>9</sup> times more rapid than that of ozone [38,39]. The overall reaction for ozone decomposition that leads to the production of hydroxyl radicals is as follows [40]:



Phenol degradation yields catechol, hydroquinone, and hydroxyl hydroquinone as first products. These aromatic intermediates transform

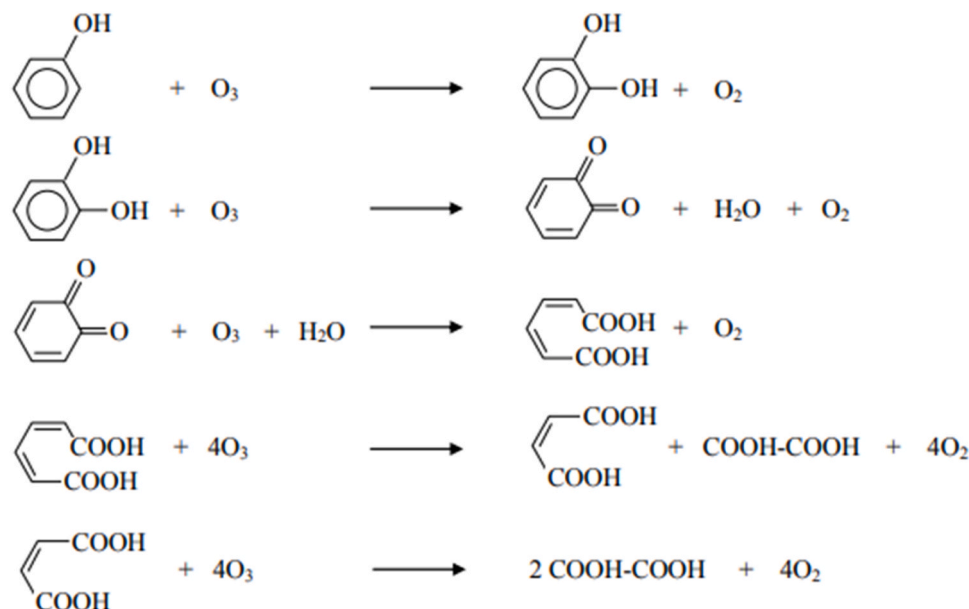


Fig. 2. Pathways of phenol degradation by ozonation reaction.

into o, p-benzoquinone, then go through ring cleavage to generate carboxylic acids like muconic acid, maleic acid, and oxalic acid, which subsequently undergo decarboxylation to liberate CO<sub>2</sub> and H<sub>2</sub>O. Fig. 3 summarizes the possible pathways of the intermediate products [41].

### 3. Results and discussion

#### 3.1. Design of experiment and central composite design

The response surface method is a statistical technique employed to design experiments in many chemical and physical processes [42,43]. Researchers have used similar methods to find better ways to get rid of pharmaceutical substances. One example is the catalytic ozonation of sarafloxacin antibiotics from water solutions, which was found to work best using response surface methodology (RSM) [44]. This research involved the design of % phenol degradation trials with the Design-Expert program, employing the central composite design (CCD) method as a component of response surface methodology (RSM). This design methodology, comparable to that employed in research on pesticide extraction techniques such as malathion [45], facilitates the adjustment of essential variables to improve system efficacy and

pollutant elimination. The desired variables were the initial concentration of phenol, air flow rate, plasma irradiation time, and applied voltage. The effects of all four variables on the % phenol degradation efficiency considered the response in this design, were investigated and modeled. Table 4 outlines the different levels at which this research examined four independent variables: power, length of time, airflow rate, and initial phenol concentration. In this study, 30 experiments were conducted using a 25 ml solution of phenol solution for each trial. The conditions and % phenol degradation for each experiment are presented in Table 5.

**Table 4**  
Low, and high levels of the independent variables investigated in this study.

Factor	Name	Units	Low actual	High actual	Low coded	High coded
A	Initial concentration of phenol	ppm	2.00	6.00	-1.00	1.00
B	Flow rate	(L/min)	0.50	1.50	-1.00	1.00
C	Time	min	5.00	15.00	-1.00	1.00
D	Applied voltage	Volt	10,000	30,000	-1.00	1.00

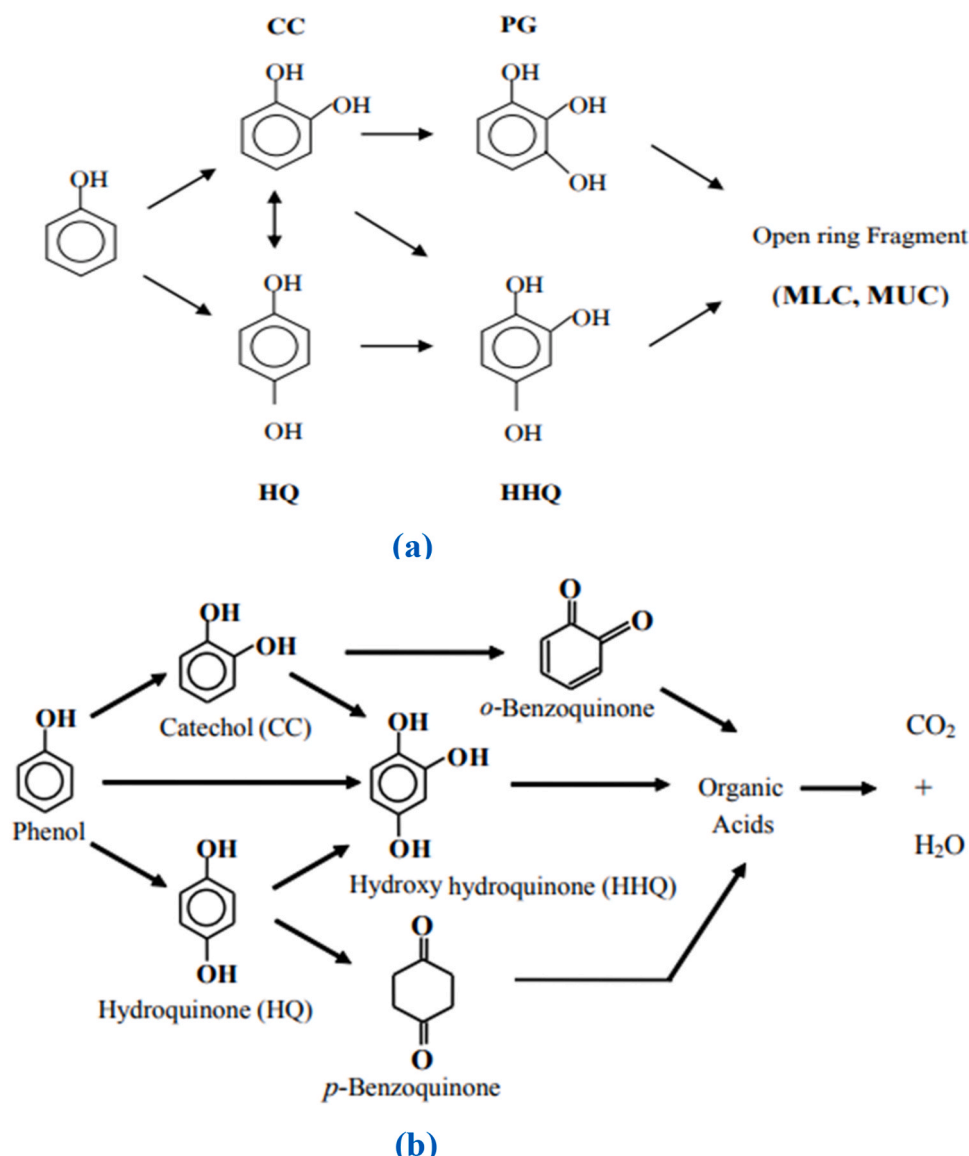


Fig. 3. Possible pathways of the phenol intermediate products.

**Table 5**  
Design data with the experimental % phenol degradation.

Run	A Initial concentration (ppm)	B Flow rate (L/ min)	C Time (min)	D Applied voltage (Volt)	% Phenol degradation
1	4	1	10	20,000	18
2	4	1	15	20,000	46.9
3	2	1	10	20,000	35
4	6	1.5	5	10,000	0
5	2	1.5	15	10,000	2.3
6	4	1	5	20,000	0
7	4	1	10	30,000	50.7
8	2	1.5	15	30,000	58
9	4	1	10	20,000	18
10	6	1.5	15	10,000	0
11	2	0.5	5	30,000	52
12	2	1.5	5	10,000	11
13	6	1	10	20,000	10
14	2	0.5	15	30,000	97.4
15	6	0.5	5	10,000	0
16	6	0.5	5	30,000	0
17	6	0.5	15	10,000	36
18	4	1	10	20,000	18
19	2	1.5	5	30,000	24
20	4	1	10	20,000	18
21	6	0.5	15	30,000	82
22	4	0.5	10	20,000	38.8
23	4	1	10	10,000	13.7
24	6	1.5	5	30,000	0
25	2	0.5	15	10,000	39
26	2	0.5	5	10,000	16
27	4	1	10	20,000	18
28	6	1.5	15	30,000	66
29	4	1	10	20,000	18
30	4	1.5	10	20,000	7

### 3.2. Statistical analysis

The best-fitting polynomial model was predicted by statistical parameters such as R-squared, adjusted R<sup>2</sup>, multiple correlation coefficients, and coefficients using Design Expert and ANOVA analysis including analysis of variance, fit statistics, model comparison statistics, coded equations, and actual equations was used to assess whether the model was significant or no significant, and the significance was based

**Table 6**  
Analysis of variance for the % phenol degradation.

Source	Sum of Squares	df	Mean Square	F Value	p-value Prob > F	
Model	18,493.54	14	1320.97	31.10	< 0.0001	significant
A- Initial concentration (ppm)	1093.56	1	1093.56	25.74	0.0001	
B-Flow rate (L/min)	2058.68	1	2058.68	48.46	< 0.0001	
C-Time (min)	5839.20	1	5839.20	137.46	< 0.0001	
D-Applied voltage (Volt)	5397.61	1	5397.61	127.06	< 0.0001	
AB	200.93	1	200.93	4.73	0.0460	
AC	514.16	1	514.16	12.10	0.0034	
AD	160.66	1	160.66	3.78	0.0708	
BC	560.51	1	560.51	13.19	0.0025	
BD	1.76	1	1.76	0.041	0.8416	
CD	1951.43	1	1951.43	45.94	< 0.0001	
A <sup>2</sup>	0.13	1	0.13	3.173E-003	0.9558	
B <sup>2</sup>	0.077	1	0.077	1.803E-003	0.9667	
C <sup>2</sup>	1.35	1	1.35	0.032	0.8609	
D <sup>2</sup>	232.45	1	232.45	5.47	0.0336	
Residual	637.19	15	42.48			
Lack of Fit	637.19	10	63.72			
Pure Error	0.000	5	0.000			
Cor Total	19,130.73	29				
Std. Dev.	6.52		R-Squared	0.9667		
Mean	26.45		Adj R-Squared	0.9356		
C.V.%	24.64		Pred R-Squared	0.7786		
PRESS	4235.31		Adeq Precision	23.355		

on calculating the F value at different probabilities.

The results in Table 6 shows that the model works well and can correctly interpret the data. The model's F-value of 31.10 signifies an unusually high level of statistical significance. This value indicates that the likelihood of obtaining a substantial F-value due to random variation is below 0.01 %, thereby affirming the model's resilience and reliability. The R<sup>2</sup> value of 0.9667 signifies that the model accounts for about 96.67 % of the variation in the data, illustrating its appropriateness and strong efficacy in characterizing degradation behavior. The adjusted R-squared value of 0.9356 substantiates this, demonstrating that the model retains its robustness after accounting for the number of variables and bolstering confidence in its predictive accuracy. The anticipated predicted R-squared value of 0.7786 indicates the model's satisfactory predictive capacity, serving as an appropriate metric in chemical analysis for variations in organic contents in industrial effluent. The precision ratio of 23.355, which is adequate, indicates a robust signal-to-noise ratio, thereby reinforcing the model's quality and predictive accuracy. The results affirm that the utilized model is useful for understanding present data and demonstrates predictive efficiency for future outcomes, rendering it a desirable instrument for industrial chemical analysis. The Regression equation in terms of actual factors of phenol degradation percentage response achieved from RSM is presented by Eq. (5).

$$\begin{aligned} \text{\% phenol degradation} = & +70.58,713 - 9.48483 \times A - 11.93933 \times B - \\ & 1.29282 \times C - 3.56586E-003 \times D + 3.54375 \times A \times B + 0.56688 \times A \\ & \times C - 1.58437E-004 \times A \times D - 2.36750 \times B \times C - 6.62500E-005 \times B \times D \\ & + 2.20875E-004 \times C \times D - 0.057018 \times A^2 + 0.68772 \times B^2 + 0.028877 \\ & \times C^2 + 9.47193E-008 \times D^2 \end{aligned} \quad (5)$$

The Model F-value of 31.10 indicates statistical significance, implying a probability of less than 0.01 % that such a high F-value would arise from random variation alone. The parameters A (Concentration), B (Flow rate), C (Time), D (applied voltage), and their interactions (AB, AC, BC, and CD) have p-values below 0.0500, indicating their considerable influence on the degrading efficiency of phenol. Insignificant factors (p-value > 0.1000) encompass BD, A<sup>2</sup>, B<sup>2</sup>, and C<sup>2</sup>, signifying their lack of substantial impact on the response variable. The model's Standard Deviation is 6.52, signifying a moderate dispersion of data points relative to the mean. An R-Squared score of 0.9667 signifies that roughly 96.67 % of the variability in the response is elucidated by

the model, indicating an excellent match.

The factors A (concentration), B (flow rate), C (time), and D (applied voltage), along with their interactions (AB, AC, BC, and CD), have p-values less than 0.0500, which means they have a big impact on how well phenol breaks down. This fits with earlier studies that used CCD and similar methods to improve processes like biosorption, showing that they could find important variables with  $R^2$  values higher than 0.95 [46, 47]. We deem these parameters essential in assessing the efficacy of the degrading process. Variables such as BD and the quadratic terms  $A^2$ ,  $B^2$ , and  $C^2$  exhibit p-values exceeding 0.1000, signifying that their impact on the response variable is statistically negligible. Therefore, we might perceive them as having an insignificant impact within this paradigm.

The model's standard deviation is 6.52, indicating a substantial dispersion of data relative to the mean. The model accounts for approximately 96.67 % of the variability in phenol degradation efficiency, according to the R-squared value of 0.9667. The elevated  $R^2$  value indicates superior alignment between the model and the empirical data obtained. Furthermore, the predicted values were plotted against the experimental data (Fig. 4). It can be seen a good relationship between the experimental and predicted values since the data points has good distribution near to the straight line suggesting that the obtained model provides a good estimation of the response.

### 3.3. Effect of the independent variables on the response variable

#### 3.3.1. Effect of initial phenol concentration on the % phenol degradation

Fig. 5 indicates a distinct inverse correlation between the initial concentration of phenol and its degradation in the cold plasma DBD reactor. Changes in phenol concentration impact the removal efficiency when we set the applied voltage at 20,000 Volt for 10 minutes, and maintain an airflow velocity of (1) L/min. A phenol degradation of 27.93 % is recorded for an initial phenol concentration of 2 ppm. Nonetheless, when the concentration rises to 6 ppm, the phenol degradation decreases to 12.34 %. The restricted presence of reactive species at elevated pollution concentrations elucidates this phenomenon. In a plasma system, reactive species such as hydroxyl radicals  $OH\bullet$ , atomic oxygen (O), and ozone ( $O_3$ ) are produced to decompose phenol molecules. At low phenol concentrations, these reactive species effectively decompose phenol, leading to increased removal rates. As the concentration escalates, the identical quantity of reactive species must engage with an increased number of pollutant molecules, resulting in a diminished percentage of degradation. This observation aligns with similar findings by Reddy's, He suggests that lower pollutant concentrations promote more efficient degradation by increasing the availability of active species relative to the quantity of pollutant molecules [48].

#### 3.3.2. Effect of air flow rate on the % phenol degradation

Fig. 6 shows how the % phenol degradation changes with different

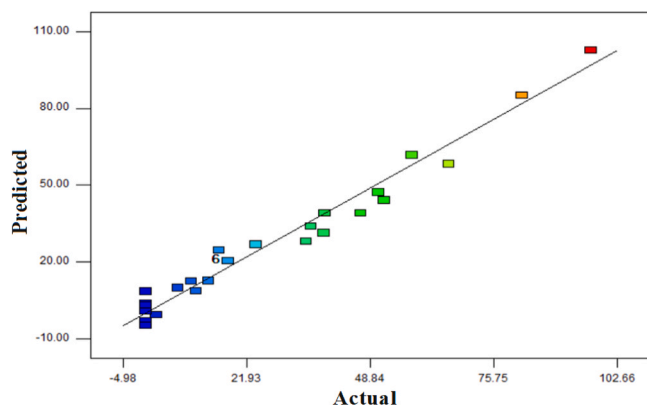


Fig. 4. The predicted versus the actual % phenol degradation.

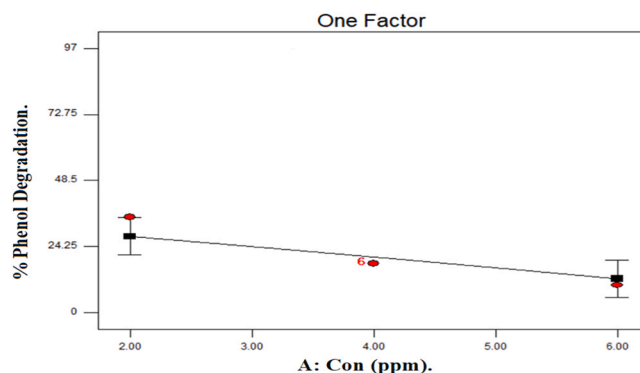


Fig. 5. Effect of initial phenol concentration on the % phenol degradation, at a constant flow rate (B) of 1 L/min, time (C) of 10 min, and applied voltage (D) of 20,000 Volt.

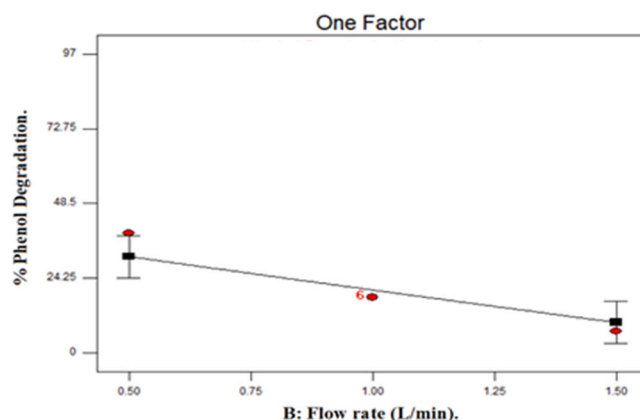


Fig. 6. Effect of flow rate on the % phenol degradation, at a constant initial phenol concentration (A) of 4 ppm, time (C) of 10 min, and applied voltage (D) of 20,000 Volt.

airflow rates. The experimental parameters were a phenol concentration of 4 ppm, a treatment period of 10 minutes, and applied voltage of 20,000 Volts, selected to investigate these effects. At an airflow velocity of 0.5 L/min, the phenol removal efficiency attained 31 %. Because there is less airflow, air can stay in the reactor for longer, which makes it easier for large amounts of ozone and reactive species, such as hydroxyl radicals, to form. These reactive species efficiently interact with phenol molecules, substantially aiding in their degradation. Higher quantities of reactive species and extended residence durations enhance the probability of effective phenol breakdown. In contrast, the phenol removal efficiency significantly decreased to 9.84 % upon increasing the airflow rate to 1.5 L/min. The decrease is due to the diminished resident time of air in the plasma reactor, resulting from the increased flow rate, which restricts the interaction length of oxygen with the plasma. When oxygen molecules enter the reactor at this faster rate, they move through the discharge zone more quickly. This makes it less likely that they will interact with the electrons and reactive particles that are made by the discharge. Thus, there is inadequate time for oxygen to transform into ozone at elevated quantities, as ozone synthesis necessitates sustained contact between oxygen and active electrons over a defined duration [49,50].

#### 3.3.3. Effect of time on the % phenol degradation

According to Fig. 7, the % phenol degradation in a DBD cold plasma reactor increases significantly as the treatment period increases. Holding the applied voltage constant at 20,000 Volt, setting the initial phenol concentration at 4 ppm, and maintaining an airflow rate of 1 L/min for

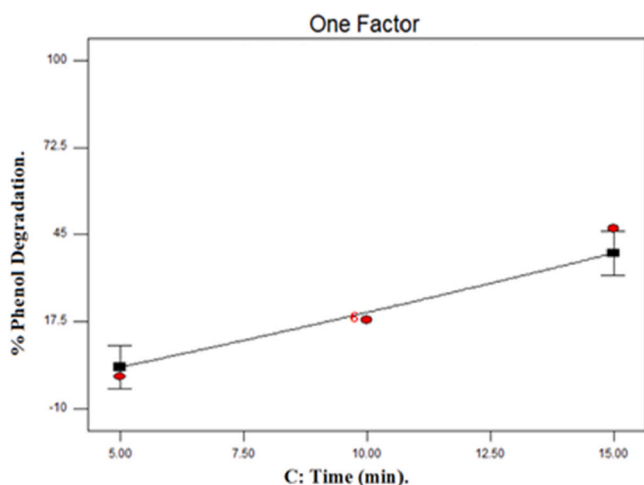


Fig. 7. Effect of time on the % phenol degradation, at a constant initial phenol concentration (A) of 4 ppm, flow rate (B) of 1 L/min, and applied voltage (D) of 20,000 Volt.

5 minutes results in a phenol degradation rate of 3.07 %. Nevertheless, this rises to 39.1 % following fifteen minutes. This proves that prolonged exposure to plasma improves degradation by increasing reactive species production. This pattern is in line with previous studies, (Iervolino et al., 2019) [51,52] found that longer treatment times led to better degradation of pollutants. Oxidation and mineralization of phenolic compounds occur gradually due to the production of reactive oxygen species in cold plasma. These species include atomic oxygen and hydroxyl radicals. The gradual breakdown of phenol was possible to note that, using the optimal operating conditions.

3.3.4. Effect of applied voltage on the % phenol degradation

Fig. 8 demonstrates the significant impact of increasing the applied voltage in the cold plasma DBD reactor on phenol degradation. By fixing the initial phenol concentration at 4 ppm, the treatment duration at 10 minutes, and the airflow rate at 1 L/min, variations in the applied voltage notably influence phenol degradation efficiency. In the initial scenario, with an applied voltage of 10,000 volts, the phenol degradation rate was 12.5 %. This lower degradation rate is attributed to the reduced generation of energetic electrons and reactive species at lower applied voltages. The primary mechanism by which phenol breaks down in cold plasma involves the generation of active species such as hydroxyl

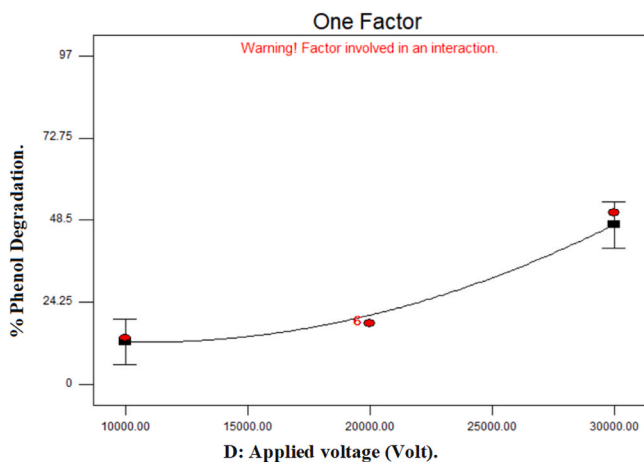


Fig. 8. Effect of applied voltage on the % phenol degradation at a constant initial phenol concentration (A) of 4 ppm, flow rate (B) of 1 L/min, and time (C) of 10 min.

radicals (OH•), atomic oxygen (O), and ozone (O<sub>3</sub>). Lower applied voltages result in a reduced production of these reactive species, leading to a slower phenol oxidation. When the applied voltage was increased to 30,000 volts, the phenol degradation rate significantly improved to 47.15 %. This increase in degradation efficiency is due to the intensified electric field, which accelerates electron collisions and enhances the generation of reactive oxygen species. These species increase the likelihood of decomposing phenol molecules into simpler byproducts, such as carbon dioxide and water [53].

3.4. Interaction effects of model parameters

The relationship between time and initial concentration, illustrated in Fig. 9, underscores the influence of both factors on phenol degradation. Degradation efficiency significantly improves when the initial phenol concentration is minimal and the treatment duration extends. This pattern shows that when concentrations are low, there are more reactive species that can interact with phenol molecules over time, making degradation easier.

Fig. 10 demonstrates the influence of both variables on phenol degradation through the relationship between applied voltage and initial phenol concentration. As the initial phenol content decreases and the applied voltage increases, the degradation efficiency is markedly enhanced. The electrical potential is crucial in chemical degradation processes. Applying a high electrical potential in a cold plasma-producing reactor produces active species, including ozone and free radicals (e.g., OH• and O•), which are potent oxidizing agents that can react with and decompose organic molecules like phenol. In addition, The DBD discharge exhibited a reduction in breakdown efficiency with increasing phenol concentration [54].

The relationship between time and air flow rate, illustrated in Fig. 11, underscores the it has also been shown that the gas flow rate affects the degradation efficiency of phenol and ozone formation [52]. For this reason, in this work, the influence of air flow rate on the degradation of phenol was investigated. The degradation of phenol as a function of run time for different air flow rate. In particular, three different air flow rates were investigated: 0.5, 0.1, and 1.5 L/min, and three different times (5,10, and 15) min with an applied voltage equal to 20,000 Volt and initial concentration of phenol (4) ppm. It was possible to note that the higher degradation of phenol was obtained at 0.5 L/min reaching a degradation equal to 56 % after 15 min of treatment. This result is very interesting compared to the literature data of (Iervolino et al., 2019) where MB discoloration, at the time of 10 min and concentration of MB 10 ppm, was equal to 92 % with 0.18 L/min and 38,000 Volt [52]. Moreover, the degradation rate decreased when the gas flow rate was increased from 0.5 up to 1.5 L/min as shown in Fig. 11. This behavior was in agreement with the literature data showing that the ozone concentration reached a maximum as a function of the air gas flow rate. So, it is possible to argue that, for this configuration, the best air

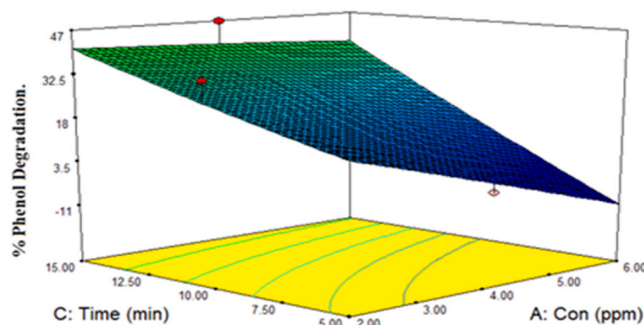


Fig. 9. Interaction effect between initial phenol concentration (A) and time (C) on the % phenol degradation at a constant flow rate (B) of 1 L/min and applied voltage (D) of 20,000 Volt.



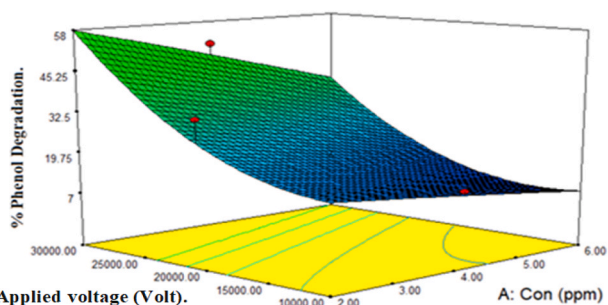


Fig. 10. Interaction effect between initial phenol concentration (A) and applied voltage (D) on the % phenol degradation at a constant flow rate (B) of 1 L/min and time (C) of 10 min.

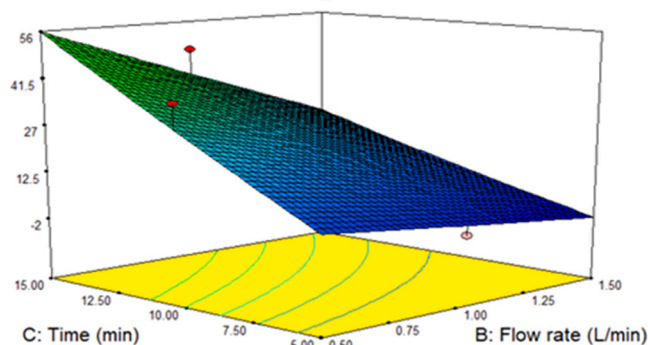


Fig. 11. Interaction effect between flow rate (B) and time (C) on the % phenol degradation at a constant initial phenol concentration (A) of 4 ppm and applied voltage (D) of 20,000 (Volt).

flow rate was 0.5 L/ min [55].

Fig. 12 indicates Enhancing both power and treatment duration produces a synergistic effect that results in elevated degradation efficiency. For instance, when operating at elevated power levels for extended periods, degradation efficiencies may reach optimal values, thereby enhancing pollutant elimination. A balance between the two parameters is essential since excessive power for a short treatment duration or insufficient power for an extended period diminishes efficiency. Studies on plasma-assisted pollutant elimination indicate that achieving efficient and economical degradation while minimizing power consumption requires optimal configurations that balance energy input.

This behavior aligns with previous research on DBD plasma reactors

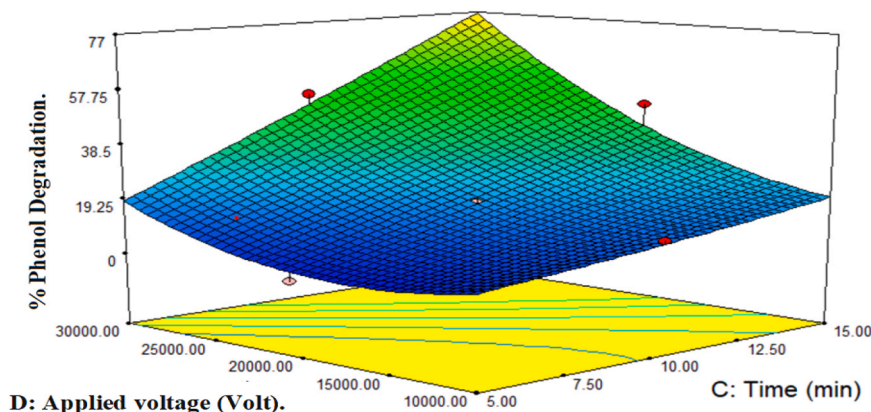


Fig. 12. Interaction effect between time (C) and applied voltage (D) on the % phenol degradation at a constant initial phenol concentration (A) of 4 ppm and flow rate (B) of 1 L/min.

for the elimination of organic contaminants. Similar results have been reported [56,57], showing that the best way to reduce degradation rates depends on how plasma operating parameters interact with each other. Response Surface Methodologies (RSM) analyze the impact of plasma procedure factors on degradation performance. The polynomial coefficients for the component degradation and ozone concentration responses exhibited remarkable linear findings ( $p < 0.001$ ) as per ANOVA. The main variables are voltage and treatment duration. They have a positive linear correlation ( $p < 0.001$ ), which means that longer treatment periods lead to better degradation.

Fig. 13 indicates that increasing the applied voltage from 10,000 to 30,000 Volt led to a significant increase in phenol degradation efficiency, rising from 2 % to 59 %. The applied voltage is the primary factor affecting the degradation process. Increasing the air flow rate from 0.5 to 1.5 L/min resulted in a slight enhancement in efficiency. Nonetheless, this effect was comparatively minor in relation to the influence of the applied voltage. Therefore, in conclusion, the applied voltage significantly influenced phenol degradation efficiency more than the airflow rate, which did not result in substantial deviations from their individual effects.

Fig. 14 illustrates the interaction effect of phenol concentration and airflow rate on degradation efficiency. The results indicate that varying phenol concentrations (2, 4, and 6 ppm) significantly influence degradation efficiency. Lower concentrations of phenol are typically associated with increased degradation percentages. At a phenol concentration of 2 ppm and a flow rate of 0.5 L/min, the system demonstrated a degradation efficiency of 97.4 %, as indicated in Run 14. Reactive species, such as hydroxyl radicals (OH) and ozone (O<sub>3</sub>), break down phenol molecules. Higher concentrations, specifically 6 ppm, make degradation less effective. For example, run 10, which used 6 ppm phenol at a flow rate of 1.5 L/min, got rid of nothing. This behavior is consistent with research indicating that elevated pollutant concentrations can impede degradation processes by competing for available reactive species. The airflow rate influences the residence time of air and reactive species in the plasma reactor, which is essential for the degradation process. In contrast, a similar configuration with a flow rate of 1.5 L/min (Run 19) achieves only 24 % degradation. Lower flow rates allow for longer residence times, which extends the time that phenol molecules interact with active radicals, ultimately improving degradation. Increased flow rates cause a rapid airflow through the reactor, which in turn shortens the residence time, potentially leading to incomplete reactions and reduced degradation efficiency. The influence of both flow rate and phenol concentration is significant. The relationship between phenol concentration and flow rate reveals an optimal condition in which decreased concentrations and lower flow rates enhance degradation efficiency. This fits with what scientists have found in the field of cold plasma: controlled flow rates and other optimized parameters make the

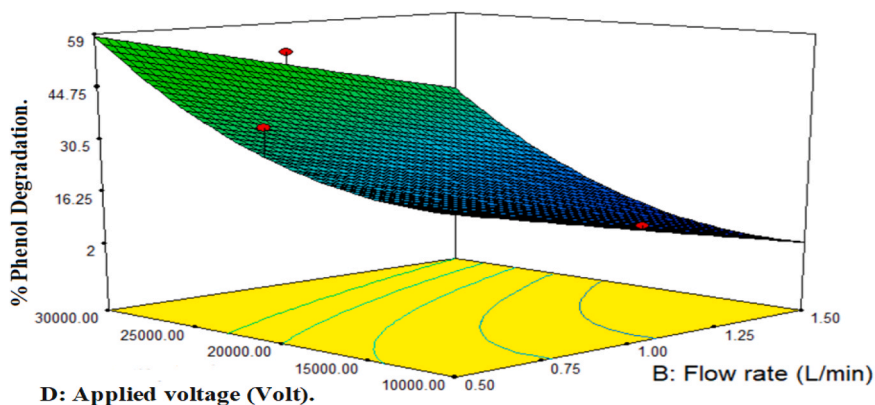


Fig. 13. Interaction effect between flow rate (B) and applied voltage (D) on the % phenol degradation at a constant initial phenol concentration (A) of 4 ppm and time (C) of 10 min.

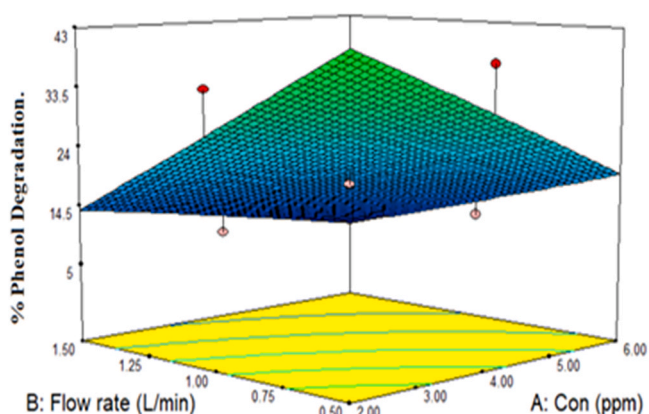


Fig. 14. Interaction effect between initial phenol concentration (A) and flow rate (B) on the % phenol degradation at a constant time (C) of 10 min and applied voltage (D) of 20,000 (Volt).

production and use of reactive species more efficient. Research backs up the idea that cold plasma reactors can break down organic pollutants at the best low flow rates by creating reactive species like ozone and hydroxyl radicals all the time [58].

Fig. 15 shows the Pareto chart for phenol degradation, where the effect strength is denoted by bar length. The time (C) has the greatest influence on the % phenol degradation, followed by applied voltage (D), flow rate (B), and initial phenol concentration (A). In the proposed model, the negative sign of the terms in Pareto charts indicates that an increase in the term causes a decrease in % phenol degradation (which is

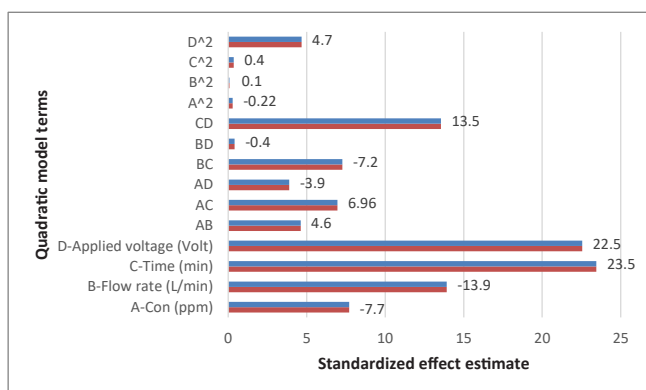


Fig. 15. Pareto chart for phenol degradation.

the case for the flow rate (B) and initial phenol concentration (A), while the positive sign of the terms indicates that an increase in the term causes an increase in the % phenol degradation (as is the case for the time (C) and applied voltage (D)).

Table 7 displays the calculated percentage contributions (PC) of each independent variable to % phenol degradation based on ANOVA results; SS is the sum of squares of these terms as determined by the equation below [59,60].

$$PC = \frac{SS}{\sum SS} \times 100 \tag{6}$$

Table 7 shows that time (C) exerts the most significant effect on the % phenol degradation. The sequence of the percentage contributions of the variables to the % phenol degradation is identical to the results shown in the Pareto charts.

### 3.5. Optimization of independent variables

To optimize the % phenol degradation, the "DESIGN EXPERT" program was employed. At an initial phenol concentration of (2.47 ppm), a flow rate of (0.50 L/min), the time (14.53 min) and applied voltage of (29,986 Volt), the maximum % phenol degradation of (97.529) was achieved (Fig. 16).

### 3.6. Comparison of % phenol degradation with similar work

In Table 8, the % phenol degradation determined in this work is compared with values recorded in previous studies. Comparing the % phenol degradation to earlier research, these findings imply that it is within an acceptable range.

## 4. Conclusion

A DBD plasma reactor has been developed for the degradation of phenol, which is considered to be toxic and present in industrial wastewater. In contrast to previous research which used electrical discharges generated in or in contact with water, phenol, was degraded through a post-discharge air plasma treatment. experiments were designed by using response surface methodology and central composite design (RSM-CCD). Four independent factors such as applied voltage, air flow rate, exposure time, and initial phenol concentration were investigated. According to the analyzed results of RSM, the experimental data is best fitted with a model of the quadratic polynomial with regression coefficient values of more than 0.9 The developed full factorial model showed that the applied voltage and treatment duration had the most significant effect on phenol degradation efficiency. At optimal degradation conditions, the applied voltage, air flow rate, exposure time, and

**Table 7**  
Percentage contributions (PC%) of the variables for % phenol degradation.

Source	(PC%)													
	A	B	C	D	AB	AC	AD	BC	BD	CD	A <sup>2</sup>	B <sup>2</sup>	C <sup>2</sup>	D <sup>2</sup>
	6.070	11.430	32.420	29.970	1.220	2.850	0.990	3.110	0.010	10.830	0.001	0.001	0.010	1.290

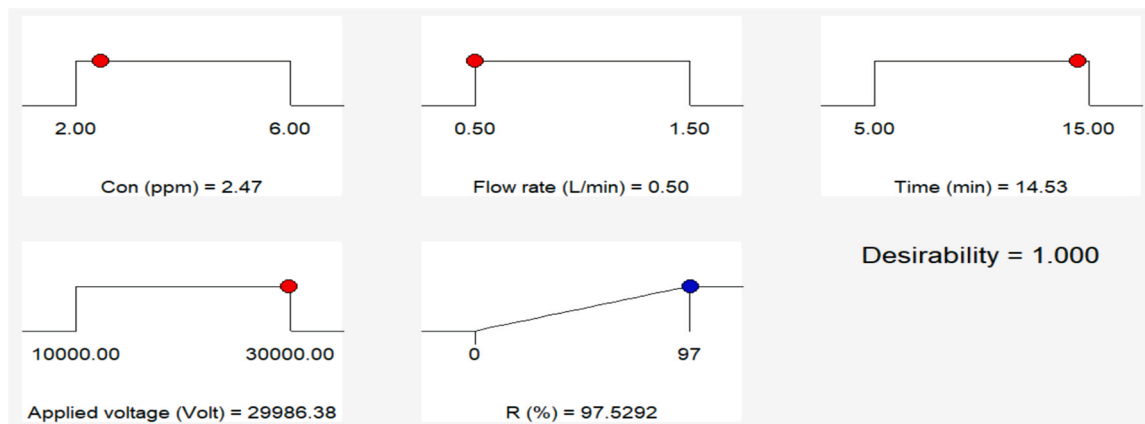


Fig. 16. Desirability ramp for the numerical optimization of four selected goals.

**Table 8**  
Comparison of the current % phenol degradation with similar work.

Reactor type	Operating conditions				Removal %	Ref.
	Initial conc. (ppm)	Power (k v)	Air flow rate L/min	Time (min)		
Dielectric barrier discharge (DBD)	50	24	20	30	98.5 %	[53]
Dielectric barrier discharge (electric discharge over water surface)	10	18	No air	100	78.8 %	[61]
Discharge reactor cylinder (CTD)	50	16	0.2	30	100 %	[62]
Single Discharge (SD)	200	0.57	0.2	30	66 %	[50]
Dielectric barrier discharge (DBD)	100	14.64	3.33 oxygen	30	90 %	[63]
Plasma reactor (DBD)	50	18	0.2	30	92 %	[48]
Plasma reactor (DBD)	2	30	0.5	15	97.4 %	Current study

initial concentration were 29,986-volt, 0.5 L/min, 14.5 minutes, and 2.47 ppm respectively. Under optimal conditions, the obtained degradation efficiency of phenol reached 97.5 % as a result of the important role of ozone and •OH radicals. The findings of the study demonstrate the potential of non-thermal plasma discharge technology as a feasible and ecofriendly approach for advanced oxidation processes and enhancing pollutant removal efficiency.

**Institutional review board statement**

Not applicable.

**Informed consent statement**

Not applicable.

**Funding**

This research received no external funding.

**CRediT authorship contribution statement**

**Rana R. Jalil:** Visualization, Validation, Resources, Methodology, Conceptualization. **Adnan A. AbdulRazak:** Writing – review & editing, Supervision, Software, Conceptualization. **Nura Nafe Ali:** Writing – original draft, Validation, Methodology, Investigation. **Haiyam M. Alayan:** Writing – review & editing, Software, Project administration, Formal analysis.

**Declaration of Competing Interest**

This is hereby declared that the manuscript entitled “**Optimization of phenol degradation through dielectric barrier discharge nonthermal plasma process towards application in industrial wastewater treatment**” Nura Nafe Ali, Haiyam M. Alayan, Adnan A. AbdulRazak and Rana R. Jalil We certify that they have NO affiliations with or involvement in any organization or entity with any financial interest or non-financial interest in the subject matter or materials discussed in this manuscript.

**Acknowledgements**

The authors are grateful to the Chemical Engineering Department, University of Technology and Petroleum Research and Development Center, Ministry of Oil, Bagdad, Iraq for providing space and facilities to conduct this work.

## Data availability

No new data was generated in this research. The data that has been used is confidential.

## References

- Ahmed FS, AbdulRazak AA, Alsaffar MA. Modelling and optimization of methylene blue adsorption from wastewater utilizing magnetic marble dust adsorbent: a response surface methodology approach. *Mater Today Proc* 2022;60:1676–88.
- Sarran MA, AbdulRazak AA, Abid MF, Jawad AD. Oily wastewater treatment using low-cost and highly efficient natural and activated Iraqi bentonite. *Desalin Water Treat* 2024;319.
- Bassim S, Mageed AK, AbdulRazak AA, Majidi HS. Green synthesis of Fe<sub>3</sub>O<sub>4</sub> nanoparticles and its applications in wastewater treatment. *Inorganics* 2022;10(12):260.
- Sarran MA, AbdulRazak AA, Abid MF, Al-Bayati ADJ, Rashid KT, Shehab MA, et al. Oily Wastewater Treatment by Using Fe<sub>3</sub>O<sub>4</sub>/Bentonite in Fixed-Bed Adsorption Column. *ChemEngineering* 2024;8:92. <https://doi.org/10.3390/chemengineering8050092>.
- Ghadhban MY, Rashid Khalid T, AbdulRazak AA, Alsally Qusay F. Recent progress and future directions of membranes green polymers for oily wastewater treatment. *Water Sci Technol* 2023;87(1):57–82. 2022.
- Durmusoglu E, Taspinar F, Karademir A. Health risk assessment of BTEX emissions in the landfill environment. *J Hazard Mater* 2010;176(1–3):870–7.
- Aziz SQ, Fakhrey ES. The effect of kawergosk oil refinery wastewater on surrounding water resources. In: *Proceedings of the first international conference on engineering and innovative technology* 2016:12–4.
- Dai X, Chen C, Chen Y, Guo S. Comprehensive evaluation of a full-scale combined biological process for the treatment of petroleum refinery wastewater using GC-MS and PCR-DGGE techniques. *Int J Electrochem Sci* 2020;15(3):2013–26.
- Saber A, Hasheminejad H, Taebi A, Ghaffari G. Optimization of Fenton-based treatment of petroleum refinery wastewater with scrap iron using response surface methodology. *Appl Water Sci* 2014;4:283–90.
- El-Naas MH, Alhajja MA, Al-Zuhair S. Evaluation of a three-step process for the treatment of petroleum refinery wastewater. *J Environ Chem Eng* 2014;2(1):56–62.
- Lawan MS, Kumar R, Rashid J, Barakat MAE-F. Recent advancements in the treatment of petroleum refinery wastewater. *Water* 2023;15(20):3676.
- Mustapha H. *Treatment of petroleum refinery wastewater with constructed wetlands*. CRC Press; 2018.
- Jafarinejad S. Activated sludge combined with powdered activated carbon (PACT process) for the petroleum industry wastewater treatment: a review. *Chem Int* 2017;3(4):368.
- Ibrahim DS, Devi PS, Balasubramanian N. Electrochemical oxidation treatment of petroleum refinery effluent. *Int J Sci Eng Res* 2013;4(8):1–5.
- El-Naas MH, Surkatti R, Al-Zuhair S. Petroleum refinery wastewater treatment: a pilot scale study. *J Water Process Eng* 2016;14:71–6.
- Khatoun K, Malik A. Cytotoxic potential of petroleum refinery wastewater mixed with domestic sewage used for irrigation of food crops in the vicinity of an oil refinery. *Heliyon* 2021;7(10).
- Aziz NM, Sabbar AA. Physicochemical properties of Basrah oil refinery discharges and its potential effects on Shatt Al-Basrah Canal. *Marsh Bull* 2013;8(1):39–57.
- Eldos HI, Khan M, Zouari N, Saeed S, Al-Ghouti MA. Characterization and assessment of process water from oil and gas production: a case study of process wastewater in Qatar. *Case Stud Chem Environ Eng* 2022;6:100210.
- Ghezali K, Bentahar N, Barsan N, Nedeff V, Moşneguţu E. Potential of *Canna indica* in vertical flow constructed wetlands for heavy metals and nitrogen removal from algeria refinery wastewater. *Sustainability* 2022;14(8):4394.
- Bastos PDA, Santos MA, Carvalho PJ, Velizarov S, Crespo JG. Pilot scale reverse osmosis refinery wastewater treatment—a techno-economical and sustainability assessment. *Environ Sci Water Res Technol* 2021;7(3):549–61.
- Nkwocha AC, Ekeke IC, Kamen FL, Oghome PI. Performance evaluation of petroleum refinery wastewater treatment plant. *Int J Sci Eng Investig* 2013;2(17).
- Daflon SDA, Guerra IL, Reynier MV, Botta CR, Campos JC. Toxicity identification and evaluation of a refinery wastewater from Brazil (Phase I). *Ecotoxicol Environ Contam* 2015;10(1):41–5.
- Fard AK, Rhadfi T, McKay G, Al-marri M, Abdala A, Hilal N, et al. Enhancing oil removal from water using ferric oxide nanoparticles doped carbon nanotubes adsorbents. *Chem Eng J* 2016;293:90–101.
- M.J. Bagajewicz, Miguel j. bagajewicz 3001, no. 2014, 2022.
- Mahmood LH, Abid MF, AbdulRazak AA, Kadhim BJ, Abdulla IN. Experimental and analysis study on removal of furfural in synthetic refinery wastewater using an agricultural waste-based modified adsorbent. *Desalin Water Treat* 2023;296:49–59. <https://doi.org/10.5004/dwt.2023.29628>.
- Aljboury D, Palaniandy P, Abdul Aziz HB, Feroz S. Treatment of petroleum wastewater by conventional and new technologies-A review. *Glob Nest J* 2017;19(3):439–52.
- Magureauu M, Piroi D, Mandache NB, David V, Medvedovici A, Parvulescu VI. Degradation of pharmaceutical compound pentoxifylline in water by non-thermal plasma treatment. *Water Res* 2010;44(11):3445–53.
- Dolatnabadi M, Ehrampoush MH, Pournamdari M, Ebrahimi AA, Fallahzadeh H, Ahmadzadeh S. Enhanced electrocatalytic elimination of fenitrothion, trifluralin, and chlorothalonil from groundwater and industrial wastewater using modified Cu-PbO<sub>2</sub> electrode. *J Mol Liq* 2023;379:121706.
- Azari A, Babaie A-A, Rezaei-Kalantary R, Esrafilii A, Moazzen M, Kakavandi B. “Nitrate removal from aqueous solution by carbon nanotubes magnetized with nano zero-valent iron,”. *J Maz Univ Med Sci* 2013;22(2):15–27.
- García MC, Mora M, Esquivel D, Foster JE, Rodero A, Jiménez-Sanchidrián C, et al. Microwave atmospheric pressure plasma jets for wastewater treatment: degradation of methylene blue as a model dye. *Chemosphere* 2017;180:239–46.
- Mohammed MJ, Khorsheed SR, Ayub SS, Ahmed TA. Treatment of contaminated collected wastewater at petroleum fuel filling stations for using as make up water for cooling tower in petroleum refineries. *J Pet Res Stud* 2023;(41).
- Khaleel OM, Dawood MM, Mohammed HA, Jameel ZI. Mathematical modeling & engineering design of wastewater treatment unit for al-kut gas filling company. *J Pet Res Stud* 2022;12(1):296–316.
- Naz MY, Shukrullah S, Ghaffar A, Rehman NU, Sagir M. A low-frequency dielectric barrier discharge system design for textile treatment. *Synth React Inorg, Met Nano Met Chem* 2016;46(1):104–9.
- Zhang FX. *Disposal and utilization of phenolic wastewater*. Beijing: Chemical Industry Press; 1983.
- Iurascu B, Siminiceanu I, Vione D, Vicente MA, Gil A. Phenol degradation in water through a heterogeneous photo-Fenton process catalyzed by Fe-treated laponite. *Water Res* 2009;43(5):1313–22.
- Eliasson B, Hirth M, Kogelschatz U. Ozone synthesis from oxygen in dielectric barrier discharges. *J Phys D Appl Phys* 1987;20(11):1421.
- Huang C-R, Shu H-Y. The reaction kinetics, decomposition pathways and intermediate formations of phenol in ozonation, UVO<sub>3</sub> and UVH<sub>2</sub>O<sub>2</sub> processes. *J Hazard Mater* 1995;41(1):47–64.
- O'Donnell C, Tiwari BK, Cullen PJ, Rice RG. *Ozone in food processing*. John Wiley & Sons; 2012.
- Zhang T, Li W, Croué J-P. A non-acid-assisted and non-hydroxyl-radical-related catalytic ozonation with ceria supported copper oxide in efficient oxalate degradation in water. *Appl Catal B Environ* 2012;121:88–94.
- Dore M, Langlais B, Legube B. Ozonation des phenols et des acides phenoxyacetiques. *Water Res* 1978;12(6):413–25.
- S. Guitonneau, J. De Laat, J.P. Duguet, C. Bonnel, and M. Dore, Oxidation of parachloronitrobenzene in dilute aqueous solution by O<sub>3</sub>+ UV and H<sub>2</sub>O<sub>2</sub>+ UV: a comparative study; 1990.
- Bassim S, Mageed AK, AbdulRazak AA, Al-Sheikh F. Photodegradation of methylene blue with aid of green synthesis of CuO/TiO<sub>2</sub> nanoparticles from extract of Citrus aurantium juice. *Bull Chem React Eng Catal* 2023;18(1):1–16. <https://doi.org/10.9767/bcrec.16417>.
- Shakor ZM, AbdulRazak AA, Shuhaib AA. Optimization of process variables for hydrogenation of cinnamaldehyde to cinnamyl alcohol over a Pt/SiO<sub>2</sub> catalyst using response surface methodology. *Chem Eng Commun* 2022;209(6):827–43.
- Dolatnabadi M, Ahmadzadeh S. Catalytic ozonation process using modified activated carbon as a catalyst for the removal of sarafloxacin antibiotic from aqueous solutions. *Anal Methods Environ Chem J* 2023;6(02):31–41.
- Yeganeh M, Azari A, Sobhi HR, Farzadkia M, Esrafilii A, Gholami M. A comprehensive systematic review and meta-analysis on the extraction of pesticide by various solid phase-based separation methods: a case study of malathion. *Int J Environ Anal Chem* 2023;103(5):1068–85.
- Azari A, Mesdaghinia A, Ghanizadeh G, Masoumbeigi H, Pirsahab M, Ghafari HR, et al. Which is better for optimizing the biosorption process of lead—central composite design or the Taguchi technique? *Water Sci Technol* 2016;74(6):1446–56.
- Alayan HM, Alsaadi MA, AlOmar MK, Hashim MA. Growth and optimization of carbon nanotubes in powder activated carbon for an efficient removal of methylene blue from aqueous solution. *Environ Technol* 2019;40(18):2400–15.
- Reddy PMK. Degradation of aqueous organic pollutants by catalytic nonthermal plasma based advanced oxidation process. *Indian Institute of Technology Hyderabad*; 2014.
- Korzec D, Freund F, Bäuml C, Penzkofer P, Nettesheim S. Hybrid dielectric barrier discharge reactor: characterization for ozone production. *Plasma* 2024;7(3):585–615.
- Farawan B, Darojatin I, Saksono N. Simultaneous degradation of phenol-Cr (VI) wastewater on air injection plasma electrolysis using titanium anode. *Chem Eng Process Intensif* 2022;172:108769.
- Iervolino G, Vaiano V, Palma V. Enhanced removal of water pollutants by dielectric barrier discharge non-thermal plasma reactor. *Sep Purif Technol* 2019;215:155–62.
- Dolatnabadi M, Ehrampoush MH, Pournamdari M, Ebrahimi AA, Fallahzadeh H, Ahmadzadeh S. Catalytic electrodes' characterization study serving polluted water treatment: environmental healthcare and ecological risk assessment. *J Environ Sci Heal Part B* 2023;58(9):594–602.
- Sahu D. Degradation of industrial phenolic wastewater using dielectric barrier discharge plasma technique. *Russ J Appl Chem* 2020;93:905–15.
- Bubnov AG, Burova EY, Grinevich VI, Rybkin VV, Kim J-K, Choi H-S. Comparative actions of NiO and TiO<sub>2</sub> catalysts on the destruction of phenol and its derivatives in a dielectric barrier discharge. *Plasma Chem Plasma Process* 2007;27:177–87.
- Songru XIE, Yong HE, Dingkun Y, Zhihua W, Kumar S, Yanqun ZHU, et al. The effects of gas flow pattern on the generation of ozone in surface dielectric barrier discharge. *Plasma Sci Technol* 2019;21(5):55505.
- Sarangapani C, Dixit Y, Milosavljevic V, Bourke P, Sullivan C, Cullen PJ. Optimization of atmospheric air plasma for degradation of organic dyes in wastewater. *Water Sci Technol* 2017;75(1):207–19.

- [57] Magureanu M, Piroi D, Mandache NB, Parvulescu V. Decomposition of methylene blue in water using a dielectric barrier discharge: Optimization of the operating parameters. *J Appl Phys* 2008;104(10).
- [58] Kumar A, Skoro N, Gernjak W, Puač N. Cold atmospheric plasma technology for removal of organic micropollutants from wastewater—a review. *Eur Phys J D* 2021;75:1–26.
- [59] Majid Z, AbdulRazak AA, Noori WAH. Modification of zeolite by magnetic nanoparticles for organic dye removal. *Arab J Sci Eng* 2019;44:5457–74.
- [60] Dolatabadi M, Ahmadzadeh S. Removal of *Staphylococcus aureus* using electro-fenton, UV/H. *Appl Water Sci* 2024;14:100. <https://doi.org/10.1007/s13201-024-02151-0>.
- [61] Wang X, Zhang G, Liu X, Hu L, Wang Q, Wang P. Effect of peroxydisulfate on the degradation of phenol under dielectric barrier discharge plasma treatment. *Chemosphere* 2019;232:462–70.
- [62] Zhang Y, Lu J, Wang X, Xin Q, Cong Y, Wang Q, et al. Phenol degradation by TiO<sub>2</sub> photocatalysts combined with different pulsed discharge systems. *J Colloid Interface Sci* 2013;409:104–11.
- [63] Hasani M, Khani M-R, Karimaei M, Yaghmaeian K, Shokri B. Degradation of 4-chlorophenol in aqueous solution by dielectric barrier discharge system: effect of fed gases. *J Environ Health Sci Eng* 2019;17:1185–94.